Pharm Res (2012) 29:198–208
DOI 10.1007/s11095-011-0535-1

RESEARCH PAPER

Linking Dissolution to Disintegration in Immediate Release Tablets Using Image Analysis and a Population Balance Modelling Approach

David Wilson • Stephen Wren • Gavin Reynolds

Received: 25 March 2011 / Accepted: 7 July 2011 / Published online: 11 August 2011

ABSTRACT

Purpose In order to achieve an improved understanding of disintegration and dissolution phenomena for an immediate release tablet formulation, a technique to monitor the number and size of particles entrained within the dissolution media was developed in combination with a population balancing model.

Methods Tablets were first characterized for crushing force, disintegration time and dissolution performance using standard USP methodologies. The performance of the tablets was then assessed using a new measurement system which links a "QicPic" particle imaging device to a USP dissolution vessel. This system enables us to measure the number and size of particles generated during tablet dissolution. The population balance mathematical model allowed a tablet erosion rate to be manipulated to fit the experimental data.

Results Results showed that tablets with differing crushing forces showed different dissolution behaviors that could be explained by differing rates of particle release into the dissolution media. These behaviors were then successfully modeled to provide a description of the dissolution and disintegration behavior of the tablets in terms of a tablet erosion rate.

Conclusions A new approach was developed that allowed the description of the dissolution behaviors of the tablets in terms of the rate that they release particles into solution. This was then successfully modeled in terms of a tablet erosion rate.

D. Wilson (✉) · G. Reynolds
Formulation Science, Pharmaceutical Development, AstraZeneca
Macclesfield, UK
e-mail: david.wilson4@astrazeneca.com

S. Wren
Analytical Science, Pharmaceutical Development, AstraZeneca
Macclesfield, UK

KEY WORDS dissolution · disintegration time · population balancing

ABBREVIATIONS

FBRM	focused beam reflectance measurement
NCE	new chemical entity
QBD	quality by design
USP	United States Pharmacopeia

INTRODUCTION

With the current industry trend for New Chemical Entities (NCEs) with poor solubility, and the new paradigm of Quality by Design (QbD), there is a need to develop measurement tools which can help improve our understanding of dissolution mechanisms. With QbD there is an emphasis on identifying critical quality attributes of the formulated product and critical processing parameters, and linking them both to clinically relevant dissolution (1). An example is the use of bio-relevant dissolution media during the development phase as a way of improving the link between *in-vitro* and *in-vivo* performance. In addition there is a focus on shifting from the current data-driven approach towards understanding dissolution from a knowledge-driven perspective. A better understanding of the rate and mechanism of dissolution can help to identify and rationalise the role of the quality attributes and process parameters. Because of this change in emphasis there is also recognition that different dissolution methods may be needed for drug product development, and for quality control purposes. Thus whilst the QC method should demonstrate the quality and consistency of the drug product, the methods used during product development may be aimed at improving

understanding of product performance. New measurement tools are needed to design and optimize formulations, and so maximize the benefit of NCEs which may have high biological activity but poor physicochemical properties.

The current and well established tests for the *in-vitro* performance of formulations are the pharmacopoeial dissolution and disintegration tests. However, whilst the dissolution and disintegration tests are useful for highlighting any performance differences (e.g. between different formulations), they are less helpful in identifying the root causes. In this paper we report initial results from a system designed to improve characterisation of the behaviour of oral immediate release tablets. Our long term aim is to gain a better insight into the link between tablet disintegration and dissolution and so gain a better understanding of overall dosage form performance. We believe that this understanding can be obtained by both the development of more integrated measurement systems, and by incorporating the experimental results into physical models with a sound theoretical framework.

With oral immediate release tablets the process of tablet disintegration is often thought of as the key step which controls dissolution, and indeed the disintegration test is sometimes proposed as a surrogate measure. For recent reviews covering the current thinking around the pharmacopoeial disintegration and dissolution tests the reader is directed to other articles (2, 3). A better understanding of the link between the disintegration and dissolution is hampered because the pharmacopoeial tests are normally carried out independently of each other and typically employ different media and hydrodynamic forces. In addition the disintegration test only provides limited information in that it is only a measure of the time required to reach a nominal end-point, i.e. that the tablet has broken into large pieces. The conventional disintegration test does not provide specific information about the rate and extent of the disintegration process, and these are important in developing a more mechanistic understanding of dosage form performance. Likewise the pharmacopoeial drug product dissolution test only measures the extent to which the drug substance has been released into solution at a limited number of time-points.

The process described somewhat loosely as drug product "dissolution" is complex and involves a number of individual steps such as hydration, erosion, primary tablet disintegration, de-agglomeration, drug substance dissolution, etc. Literature covering some of these steps already exists. For example the impact of the degree of drug substance agglomeration on the dissolution rate has been studied by the use of dynamic laser diffraction measurement (4–6). In separate work focused beam reflectance measurement (FBRM) has been used to monitor the rate of particle generation from a dissolving dosage form (7, 8). In the laser diffraction studies the overall dissolution rate was measured by UV absorbance and the data fitted to a model which assumed contributions due to both dispersed drug substance particles, and agglomerates of the particles (including the tablet surface). An important feature of the model was the much greater dissolution rate from the dispersed particles than from the agglomerates. The degree of particle agglomeration was measured as a function of time and good agreement was found between levels obtained from UV absorbance and those from the laser diffraction measurement. In more recent work the reduction in intensity of scattered laser light was used as a measure of the dissolution rate of pharmaceutical powders (9).

In this paper we build upon the laser diffraction and FBRM studies by using optical imaging and population balance modeling. This allows us to model the dissolution behavior in terms of tablet disintegration, particle dispersion, and erosion rates. The benefit of dynamic optical imaging is that it allows the assessment of not only the particle size distribution, but also the number of the particles and their shape with time. This in turn through the population balance modeling can allow an inference of the true rate of tablet disintegration. In this paper we will show that the net drug product dissolution rate (i.e. that which is measured in the pharmacopeial method) is a function of both the rate at which particles are generated by disintegration processes, and the rate at which particles are eroded and removed by dissolution processes.

In order to provide a more comprehensive analysis of *in vitro* tablet performance, we consider both tablet disintegration and dissolution in terms of mechanisms, processes, and reaction rates, rather than as simple measures of extent as defined by standardized testing methods. In particular we show how it is important to consider the rate limiting step governing dosage form performance. To illustrate this concept we show how two different dissolution profiles can be generated by two batches of the same formulation which have been engineered to have different disintegration behaviours. The experimental observations are also consistent with expectations from an *in-silico* reaction rate model based upon the population balance modeling.

MATERIALS AND METHODS

Materials

Two batches of uncoated tablets were prepared using high shear wet granulation. The tablets were engineered to have differing physical properties. Specifically, the wet granulation and compression processes were altered to provide tablets with differing crushing forces.

The tablets were prepared from the same starting formulation. Containing 5%w/w drug substance, 15%w/w insoluble excipients and 80%w/w soluble excipients.

Methods

Standard Analytical Methods

The crushing force was determined using a 6 D tablet tester (Copley, UK) with 6 tablets per batch analysed.

Disintegration time of the tablets was measured following the standard USP methodology. This involved assessing the time required for all fragments of a tablet to fall through a 2 mm square mesh of an agitated basket. This was achieved with a ZT2/2 apparatus (Erweka, Germany), operating with water warmed to 37°C. In a departure from the standard USP methodology, an average disintegration time of 6 tablets is shown in the results rather than the time taken for the final tablet of 6 to disintegrate.

Dissolution testing in 500 ml of pH 1.4 NaCl (2 g/l)/HCl dissolution medium was performed using an automated AT70 Smart dissolution bath with UV finish (Sotax, Switzerland), taking an average of the percentage dissolution of 6 tablets. The paddle speed was 60 rpm and the extent of drug substance dissolution at times of 5, 10, 20, 30, 45, and 60 min was determined by comparing the UV absorbance at 343 nm with that of a drug substance reference standard.

The mass mean particle size of the drug substance was measured by laser diffraction using a Sympatec Helos apparatus (Sympatec, Germany). Utilising the Rodos dry powder dispersion apparatus.

The mass mean particle size of the soluble and insoluble excipients were measured by QicPic image analysis using a Sympatec QicPic apparatus (Sympatec, Germany). Utilising the Rodos dry powder dispersion apparatus.

Novel Dissolution Testing Apparatus

As discussed in the introduction the objective of this work was to improve understanding of disintegration and dissolution processes by measuring the evolution and loss of particles. Previous approaches are not ideal as laser diffraction doesn't give information on the number of particles, and FBRM probes are prone to fouling from any adhesive particles (10–12). We use a conventional dissolution vessel linked to the QicPic image analyser.

The QicPic dynamic image analyser is commonly used to measure the particle size and shape of dry powders and granular materials within the pharmaceutical industry (13, 14). In this application, the QicPic was combined with a liquid dispersion system the "Lixell" unit (Sympatec, Germany) connected to a standard USP dissolution vessel. Our testing system reproduces the conditions used by the standard dissolution system discussed previously (identical paddle speed and position, volume of dissolution media etc). Particles were removed from the dissolution vessel using a peristaltic pump operating at a pumping rate of 235 ml/min, with the goal of transporting a representative sample of any entrained particles to the QicPic. The stream was passed through the QicPic with all particles imaged at a rate of 25 frames/s before being returned to the dissolution bath. Inlet and outlet positions of the stream were positioned just below the dissolution bath paddle which was set to a height of 2.5 cm and revolved at 60 RPM. The QicPic was configured to image for 2 min periods for a total time of 62 min and all images were analysed using Windox 5 software (Sympatec, Germany). A schematic of the apparatus can be found in Fig. 1 and an example of the images made available by the QicPic is shown in Fig. 2.

The data sets were analyzed in terms of both absolute particle number and volume weighted particle size distributions.

RESULTS

Results from the tablet crushing force and standard disintegration testing are given in Table I, drug substance particle size, soluble excipient and insoluble excipients particle size are given in Table II. The results of the standard dissolution testing are given in Fig. 3.

Both the standard dissolution (Fig. 3) and standard disintegration (Table I) test show a clear difference between the *in-vitro* performance of the tablets, with tablet A dissolving and disintegrating much faster than tablet B. Differences are also shown in the hardness of the two tablets (Table I) with tablet B being harder than tablet A. Tablet A, which has a rapid standard disintegration time of 100 s, gives a dissolution profile characterized by a fast initial rate of release and then a slower phase which reaches about 95% after 60 min. Tablet B, which has a standard disintegration time of 600 s, shows a sigmoidal dissolution

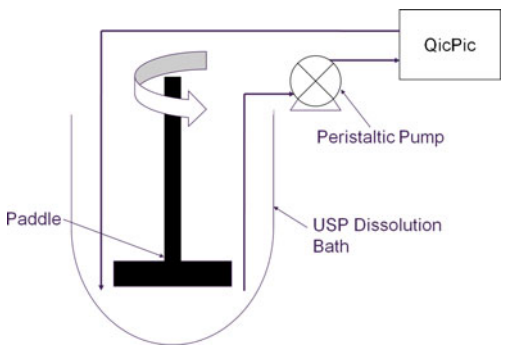

Fig. 1 Diagram of the novel dissolution testing apparatus.

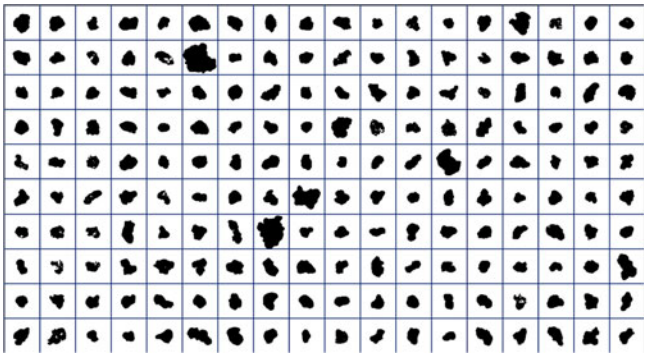

Fig. 2 Example of the imaging capability of the QicPic, showing projected images of individual particles the boundary of each box is 400 μm.

profile with a slow initial rate followed by a faster rate and then a second slow asymptotic phase, reaching about 75% drug release after 60 min. At a qualitative level the link between a slower tablet standard disintegration and slower dissolution is not surprising, but a detailed mechanistic understanding of the differences can be obtained by measuring the number and sizes of the particles and modeling their generation and loss.

The use of the QicPic image analysis technique, allows for the assessment of both the number and the size of particles entrained in solution as a function of time. The change in absolute particle number, and the mass weighted particle size distribution plots are presented in Figs. 4 and 5 respectively. In addition, the volume weighted D50 values obtained are shown in Fig. 6.

Upon analysis of the particle size and number data from tablets A and B, clear differences were seen, with tablet A releasing particles at a far greater rate than tablet B (Fig. 4). It was also seen that in the particle release profile of tablet A (Fig. 4), the maximum number of particles was obtained after only 5 min whilst for tablet B a maximum was not reached until approximately 30 min. Figure 4 also shows that with tablet A the number of particles decreases after the maximum value at 5 min. The shape of the decline suggests a trend towards a constant number of particles, and this is to be expected as the formulation contains several insoluble components (15%w/w). With tablet B the number of particles also appears to decline after 30 min although the trend is much less clear (140 particles/min) than with tablet A (860 particles/min).

As the quantitative formulation for both tablets is the same, it would be expected that they should eventually

Table I Summary of the Physical Characterisation of the Tablets

	Tablet A	Tablet B
Crushing force (N)	80	111
Mean disintegration time (s) [USP method]	100	579

Table II Summary of Particle Size Analysis of the Tablet Components

	Drug Substance	Soluble Excipient	Insoluble Excipient
D50	5	170	80
D90	13	480	160

reach the same value of remaining entrained particles. However, from Fig. 4, it appears that the two tablets asymptote to different total numbers of entrained particles. It is not clear whether the differences are just due to the slower rate of particle dissolution from tablet B or whether there are differences in the degree of agglomeration of insoluble particles. Whatever the difference it is clear that there is a strong link between the rate of change in the number of suspended particles and the rate of dissolution. The slope of dissolution curves in Fig. 3 implies that dissolution is continuing at 60 min for both tablets, but is much more complete (hence a shallower slope) for tablet A.

The mass weighted size distributions of the particles generated during the dissolution of tablets A and B are shown in Fig. 5. The benefit of examining the particle size distribution is that we can follow the different changes occurring to the different size ranges. Thus whilst similar particle size ranges were obtained from both tablets different changes occurred to these different ranges. Figure 5 shows that for tablet A the ratios of the peaks changes with time, with the peak at approximately 10 µm shrinking (top right hand image) whilst the peak at 90 µm remains almost constant (top left hand image). With tablet B the ratio of the peaks changes less over time. The 10 and 90 µm peaks are in the approximate positions expected from the drug substance and the insoluble component of the formulation (Table II). Thus we interpret the decline of the 10 µm peak to arise from the dissolution of dispersed drug substance particles.

The D50 values for the volume weighted cumulative distributions of both tablets can be seen in Fig. 6, which

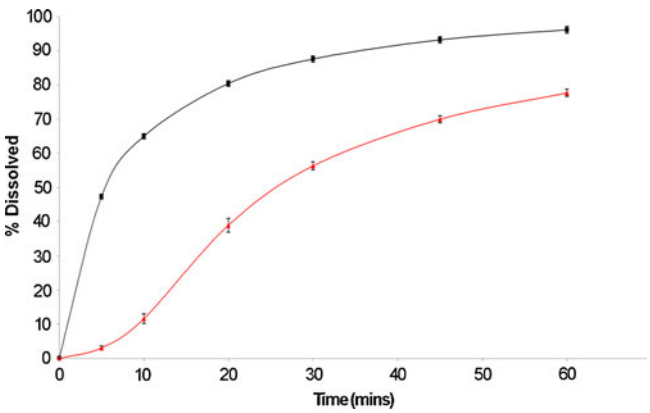

Fig. 3 Standard dissolution testing of the tablet batches showing *tablet A* (*black trace*) and *tablet B* (*red trace*).

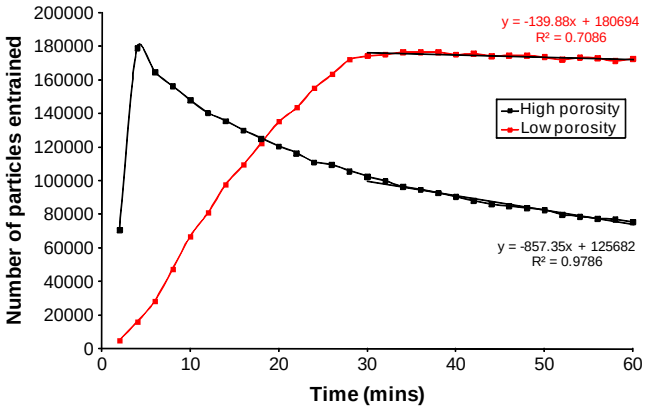

Fig. 4 Particle number with the progression of time for *tablet A* (*black trace*) and *tablet B* (red trace).

shows a scatter in the D50 values as a function of time, but regression of the data indicates a constant D50 value for tablet A whilst with tablet B the D50 value reduces in size as the dissolution continues. This could indicate the presence of a secondary size reduction step in the dissolution process of tablet B.

DISCUSSION

Novel Dissolution/Disintegration Method

Clearly tablets A and B are exhibiting differing behavior, both in terms of their dissolution profiles (Fig. 3) and in releasing particles at different rates (Fig. 4). In an attempt to correlate the two phenomena we considered the rate of dissolution in addition to the extent. The standard dissolution traces were differentiated to determine the dissolution rates and these were plotted on the same graph as the particle release profiles (Fig. 7). It can be seen that

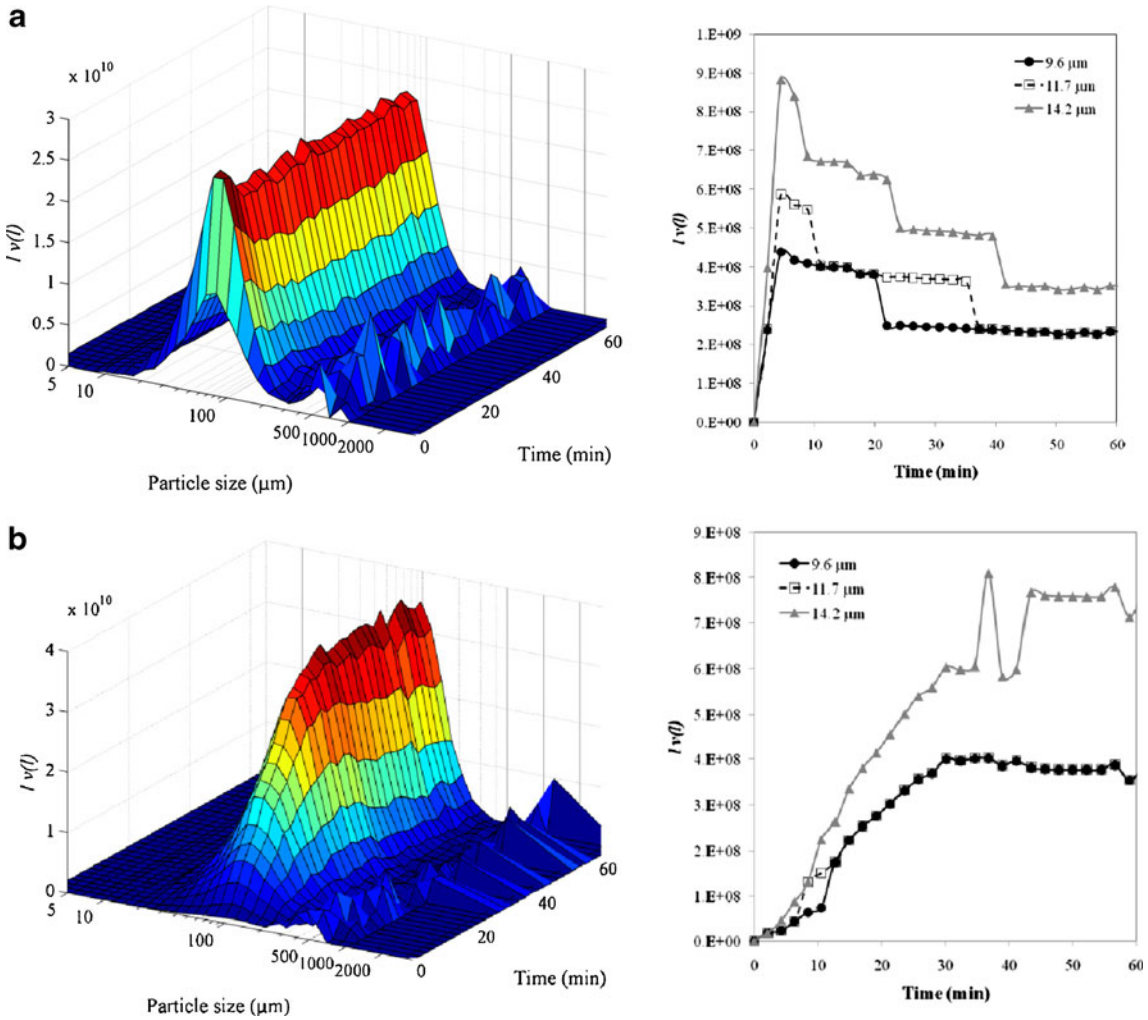

Fig. 5 Mass weighted particle size distributions of *tablet A* (*top images*) and *tablet B* (*bottom image*). *Left side images* show the total distribution; *right side images* show three small size classes in the approximate location of the drug substance.

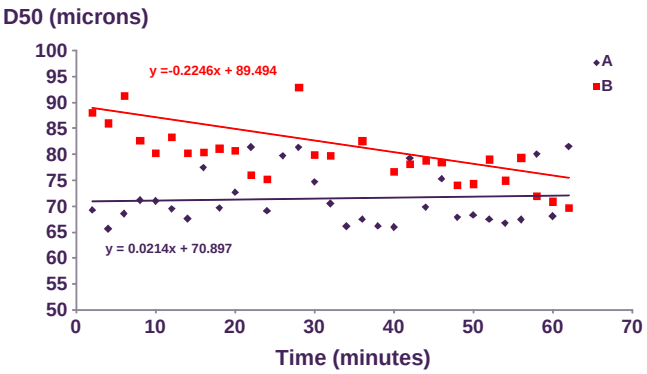

Fig. 6 Volume weighted D50 values with time for *tablet A* (*black trace*) and *tablet B* (*red trace*).

the shape of the particle release profiles and the first differential of the dissolution plots closely follow each other for rank order. That is, the tablet with a faster rate of dissolution tends to have a larger number of particles entrained in solution. As the rate of dissolution of the drug substance should be proportional to the available surface area of the particles, we propose that the rate of drug substance dissolution is in general proportional to the number of particles entrained in solution and as such is a function of the rate of particle release from the tablets.

In the standard disintegration test, the tablet is defined as having disintegrated when the entire tablet mass has passed through a 2 mm square mesh (15). The approach developed here allows for an alternate definition of disintegration, namely when the particles entrained in solution reach a maximum value. This alternative view is based upon a consideration of disintegration as a finite process rather than a singular event, and allows for the fact that tablet disintegration is not instantaneous but can occur on a timescale of minutes. Consideration of disintegration as a process is important as otherwise it is difficult to reconcile inconsistencies in conventional wisdom, i.e. that a process (dissolution) could be adequately described by a single event (disintegration).

The standard disintegration test would indicate that the difference between the disintegration times of the two tablets would be approximately 500 s (Table I). However, the particle release profiles (Fig. 4) show that the difference in the time required for the maximum number of entrained particles to be obtained to be ~1200 s. As the method developed here allows for both the measurement of dissolution and disintegration simultaneously, it is proposed that the value of 1200 s is a far more accurate measurement of the performance difference between the tablets caused by the physical differences imparted by the process.

Modeling Tablet Disintegration and Dissolution

A key aspect of this work is the development of a model which covers both the tablet disintegration and drug substance dissolution processes. We suggest that consideration of the differing dissolution profiles (Fig. 3) combined with the rate of change of the number of particles as a function of time (Fig. 4) show two key dissolution mechanisms: intrinsic drug substance dissolution rate limited and disintegration limited dissolution. This is shown schematically in Fig. 8.

Tablet A initially releases a large number of particles into suspension due to rapid disintegration. During this intial phase the rate of particle generation is greater than the rate at which they are lost. After primary tablet disintegration is complete there is no longer significant generation of new particles and the total particle count reduces as the soluble components dissolve.

Tablet B releases particles into suspension slowly over time. The number of particles systematically increases to a

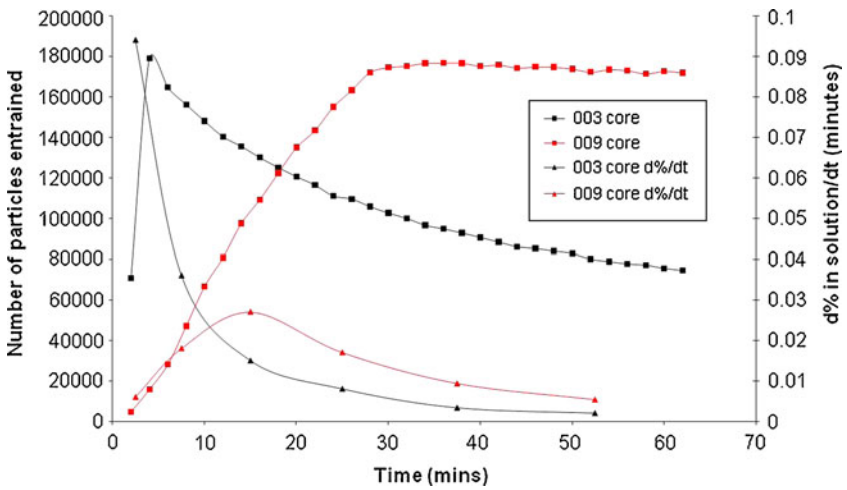

Fig. 7 Particle release profiles and the first differential of the dissolution profiles for *tablet A* (*black trace*) and *tablet B* (*red trace*).

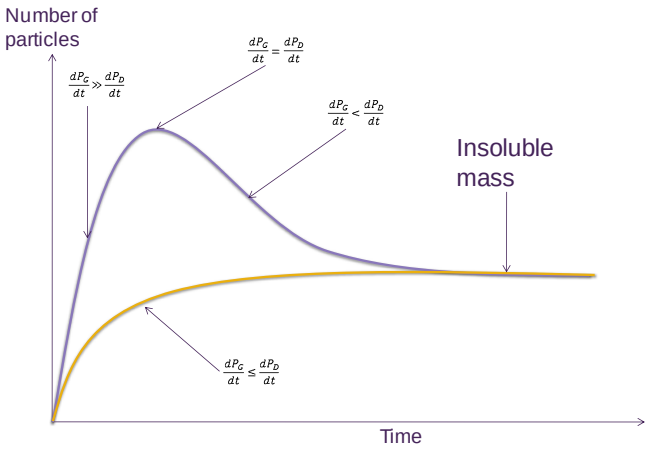

Fig. 8 Number of particle with time for scenarios involving differing rates of particle generation from a tablet (dP_g) and particle dissolution (dP_D) with time (dt).

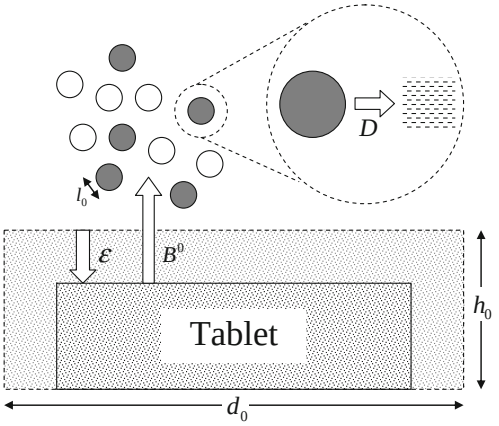

Fig. 9 Schematic diagram of simplified eroding tablet showing key dimensions with the time parameter in subscript and rate processes.

plateau, representing the particle count of insoluble components. The soluble components dissolve at the solution interface of the tablet, or from the released particles as soon as they are generated. To summarise the dissolution process exhibited by Tablet B is dominated by a slow erosion limited release of particles.

The three-dimensional mass size distributions in Fig. 5 show the relative changes in total mass of particles. In particular, the reduction in the mass of smaller particles in tablet A is indicative of the initial fast release and subsequent dissolution of the drug substance. There is not a corresponding reduction in the smaller sizes for tablet B, indicating that soluble particles dissolve at the rate of release or faster and therefore only the particle size of insoluble components is shown. This is consistent with the observations that the dissolution release from this tablet is disintegration limited.

Population Balance Modeling

A simplified population balance model of tablet disintegration and dissolution was developed in order to explore the competing rates of particulate release from the tablet and dissolution. Consider the schematic diagram of an eroding tablet as shown in Fig. 9. This diagram depicts a cylindrical tablet eroding with an isotropic linear erosion rate of ε. As a result of this erosion, particles are released into solution at a rate of B^0. Once in solution, soluble particles can then dissolve at a rate of D. This mechanistic description will now be developed into a numerical description.

As the surface of the tablet erodes due to water ingress and shear at the surface, particulate matter is released into the bulk dissolution media. Assuming a cylindrically shaped tablet and a linear erosion rate, ε, the volume of the tablet as a function of time, t, will be:

$$V_t(t) = \frac{\pi}{4}(d_0 - 2\varepsilon t)^2(h_0 - 2\varepsilon t) \tag{1}$$

The rate of volume of material released from the tablet due to erosion can then be determined by taking the differential:

$$V_t'(t) = \frac{\pi}{4}\left(2\varepsilon(d_0 - 2\varepsilon t)^2 + 4\varepsilon(d_0 - 2\varepsilon t)(h_0 - 2\varepsilon t)\right) \tag{2}$$

To model the change in the particle size distribution during dissolution, a population balance model will be utilised. The population balance equation is a generalized rate-based equation for modeling the temporal rate of change of particles as a function of size and/or other properties. Population balance equations have been used for many years for modeling particle rate processes in many different systems, including crystallization (16) and agglomeration (17). To model the rate of release and dissolution of each component of the tablet (drug substance—subscript a, soluble excipient—subscript e,s and insoluble excipient-subscript e,i) from the tablet, the following simultaneous population balance equations will be used to describe the number size distribution, n, of each component:

$$\frac{\partial n_a}{\partial t} = B_a^0\delta(l - l_{0,a}) + D_a\frac{\partial n_a}{dl} \tag{3}$$

$$\frac{\partial n_{e,s}}{\partial t} = B_{e,s}^0\delta(l - l_{0,e,s}) + D_{e,s}\frac{\partial n_{e,s}}{dl} \tag{4}$$

$$\frac{\partial n_{e,i}}{\partial t} = B_{e,i}^0\delta(l - l_{0,e,i}) \tag{5}$$

Here, δ is the Dirac delta function and the rate of release of particles from the eroding tablet into the dissolution media is captured by the rate terms, B_a^0, $B_{e,s}^0$, *and* $B_{e,i}^0$. To

maintain the simplicity of the model, particles are released monodispersed at the sizes given by $l_{0,a}$, $l_{0,e,s}$ and $l_{0,e,i}$, although in practice a distribution could be used. The dissolution of the drug substance and soluble excipient particles is denoted by the dissolution rate terms, D_a and $D_{e,s}$, respectively. Assuming dissolution is diffusion limited, the following expression is used:

$$D = \frac{\mathrm{D}v_m}{Ml}\left(S - S^*\right) \tag{6}$$

where D is the diffusion coefficient, v_m is the molar volume, M is the molecular mass, S is the solution concentration and S^* is the solubility.

The primary aim of developing this model is to mechanistically capture the key features observed from the experimental work. Therefore, although not necessary, the following assumptions will be made in order simplify the subsequent equations. All material within the tablet will be assumed to have approximately the same density. Additionally, all particles released from the tablet will be assumed to have the same average size and shape. Based on these assumptions, the release rate of numbers of particles of active, soluble excipient and insoluble excipient can be described as:

$$B_a^0 = \frac{x_a V_t'(t)}{\phi\, l_{0,a}^3} \quad B_{e,s}^0 = \frac{x_{e,s} V_t'(t)}{\phi\, l_{0,e,s}^3} \quad B_{e,i}^0 = \frac{x_{e,i} V_t'(t)}{\phi\, l_{0,e,i}^3} \tag{7}$$

Where x is the mass fraction of each component and ϕ is the particle shape factor.

A discretised method was utilised to solve the population balance equations (Hounslow, 1988). Essentially, with this approach each temporal size distribution is discretised into a geometric progression of size classes where $L_{i+1}/L_i = r$. This reduces each population balance equation into a system of ordinary differential equations that need to be solved to find the number of particles in size class i as a function of time, $\mathcal{N}_i$. The expression for the dissolution rate term is derived as follows. In time dt a number of particles, $d\mathcal{N}_{in}$ will dissolve into the ith size range from the $(i+1)$ size range:

$$d\mathcal{N}_{in} = D(L_{i+1})n(L_{i+1})dt = D_{i+1}\frac{\mathcal{N}_{i+1}}{L_{i+2} - L_{i+1}}dt \tag{8}$$

Similarly a number of particles will dissolve out of the ith interval into the (i-1)th interval:

$$d\mathcal{N}_{out} = D_i\frac{\mathcal{N}_i}{L_{i+1} - L_i}dt \tag{9}$$

The overall rate is given by

$$\begin{aligned}\frac{d\mathcal{N}_i}{dt} &= D_{i+1}\frac{\mathcal{N}_{i+1}}{L_{i+2} - L_{i+1}} - D_i\frac{\mathcal{N}_i}{L_{i+1} - L_i} \\ &= \frac{1}{(r-1)L}\left(\frac{D_{i+1}\mathcal{N}_{i+1}}{r} - D_i\mathcal{N}_i\right)\end{aligned} \tag{10}$$

In addition to solving the population balance equations, continuity equations are required in order to quantify the solution concentrations of the drug substance and soluble excipient. The continuity equation for the drug substance is assembled as the difference between the mass of drug substance released from the tablet and the total mass of the undissolved drug substance particles:

$$s_a(t) = x_a\rho\frac{(V_t(0) - V_t(t))}{V_m} - \rho\phi_a m_{a,3}(t) \tag{11}$$

Here, $m_{a,3}(t)$ is the third moment of the drug substance size distribution at time t and ρ is the density of the drug substance. Expressed in a discretised form, the third moment is given by:

$$m_{a,3}(t) = \sum_i l_i^3\mathcal{N}_i \tag{12}$$

Similarly a continuity equation is constructed for the soluble excipient. The system of discretised equations were solved using Matlab (v 7.9.0.529, The MathWorks).

Table III Constants Used for Parametric Simulation and Experimental Data Fitting

Symbol	Parameter Description	Value for parametric simulation	Value for experimental data fitting	Units
$d(0)$	Tablet diameter	10	7	mm
$h(0)$	Tablet thickness	5	3	mm
Vm	Volume of dissolution media	500	500	ml
ϕ	Particle shape factor	π/6	π/6	–
x_a	Mass fraction of active component	50	5	%
$x_{e,s}$	Mass fraction of soluble excipient	0	80	%
$\frac{D_a v_{m,a}}{M_a}$	Lumped diffusion parameter for drug substance	1×10^{-10}	1×10^{-10}	$m^5kg^{-1}\ s^{-1}$
$\frac{D_{e,s}v_{m,e,s}}{M_{e,s}}$	Lumped diffusion parameter for soluble excipient	–	1×10^{-9}	$m^5kg^{-1}\ s^{-1}$
S^*_a	Solubility of drug substance	0.35	0.017	mg/ml
$S^*_{e,s}$	Solubility of soluble excipient	–	10	mg/ml
l_0	Particle size	100	See Table IV	μm

Influence of Time to Complete Disintegration on Dissolution and Particle Generation

In order to facilitate discussion a new parameter, termed the time to complete disintegration, will be introduced. This is essentially the time taken for complete erosion of the smallest tablet dimension. Assuming an equal erosion rate on each surface of the tablet, this can be expressed as:

$$t_\varepsilon = \frac{\min[d(0), h(0)]}{2\,\varepsilon} \qquad (13)$$

Simulation Using the Model

To visualise the influence of changing the erosion rate on the number of particles and the rate of dissolution, the behaviour of a hypothetical tablet with the properties listed in Table III was simulated. The solubility was selected such that the tablet would be just completely soluble in the media. The time to complete disintegration was then varied.

Figure 10 shows the dissolution profiles, and Fig. 11 the number of suspended particles, for time to complete disintegration scenarios ranging from 1 to 100 mins. As the time to complete disintegration increases (i.e. the erosion rate constant decreases), there is a retardation in the initial rate of dissolution. The graph showing the number of suspended particles (Fig. 11) is more complex and reflects the different rates at which particles are

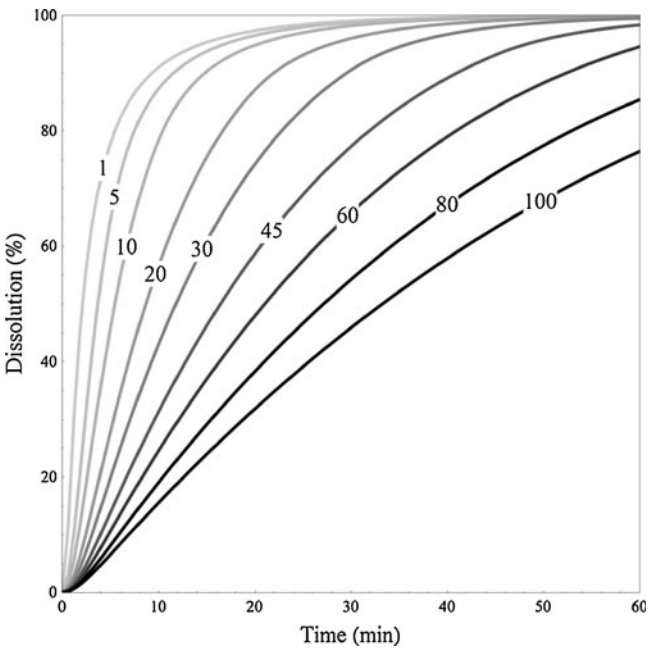

Fig. 10 Dissolution profiles for differing time to complete disintegration scenarios (time in minutes on curve).

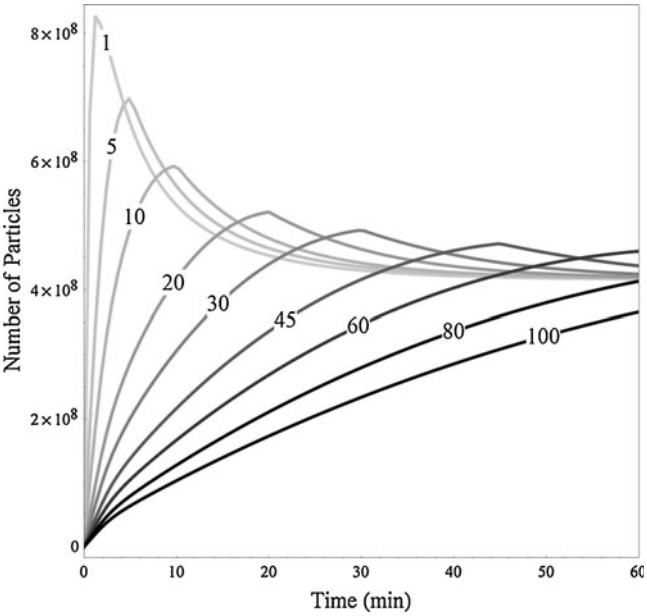

Fig. 11 The number of suspended particles with the differing time to complete disintegration scenarios (time in minutes on curve).

generated, and the rate at which the soluble particles dissolve. For low values of the time to complete disintegration there is an initial peak in the number of particles followed by a gradual decline. As the time to complete disintegration increases this peak becomes less pronounced and moves to later time points.

Fitting to Experimental Data

The model was fitted to experimental data in order to assess its ability to describe the dissolution behaviour and also to determine the time to complete disintegration. The dissolution data for tablets A and B were fitted using the model constants given instable III. Four unknown parameters were adjusted to fit the data: the times for complete disintegration for the two tablets and the initial particle sizes in both cases. The three

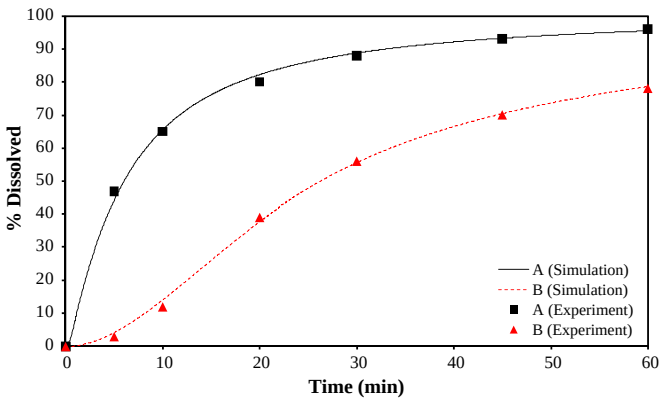

Fig. 12 Measured and simulated dissolution profiles for tablets A and B.

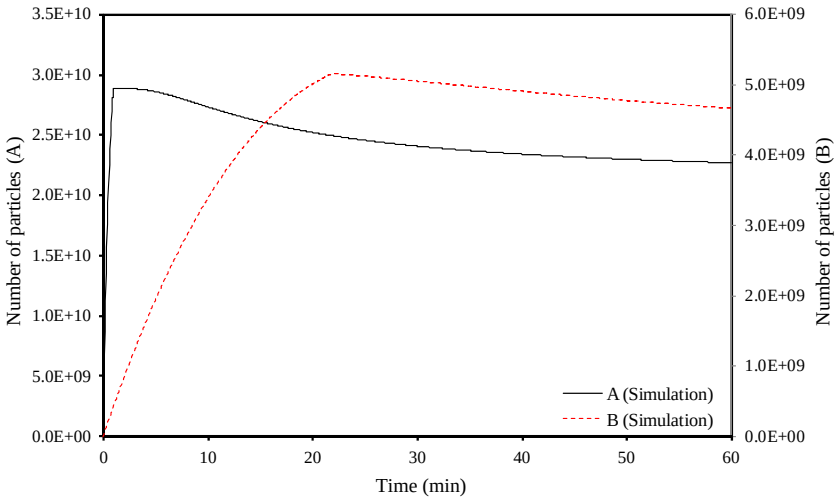

Fig. 13 Simulated number of particles during dissolution of tablets A and B.

parameters were estimated by minimising the following objective function:

$$\chi^2(\mathbf{y}) = \sum_i \left[D_{\mathrm{A},i} - D_{\mathrm{Apred},i}\right]^2 + \sum_i \left[D_{\mathrm{B},i} - D_{\mathrm{Bpred},i}\right]^2$$

where **y** is the list of parameters and D_i is the dissolution percentage at time step i. The fitted parameters are shown in Table I Summary of the physical characterisation of the tablets

A graphical comparison of the dissolutions profiles is provided in Fig. 12. For both tablet A and tablet B the dissolution profiles are quantitatively described very well, with R^2 values of greater than 0.99. The simulated number of particles is shown in Fig. 13. Comparing this with the measured number of particles (Fig. 4) shows some qualitative similarity for both tablets. For tablet A, the simulated number of particles exhibits a less distinct maximum than is observed in practice. Qualitatively, the number of particles generated during the simulation of tablet B compares favorably with the measured particle numbers (Fig. 4), showing a gradual increase in number, followed by a very gradual decrease. The fitted times to complete disintegration (Table I Summary of the physical characterisation of the tablets Table IV) indicate that tablet B takes considerably longer to disintegrate than tablet A. Additionally, the fitted parameters indicate a difference in the initial particle sizes released from the tablets during the simulation. In the simplistic model developed, the assumption is that primary particulate material is released from the tablets. Practically, processing or storage conditions may alter the particle size of the formulation components although the underlying API particle size may be expected to be similar between the two tablets. Figure 6 shows that the measured particle sizes at the start of the dissolution of each tablet are different. This suggests that although there is a clear difference in the time to complete disintegration between the two tablets, there is also a secondary mechanistic difference that is not described by the model, but has been approximated by using a different initial particle size released from the eroding tablet. This secondary mechanism could be due to de-agglomeration or secondary erosion. As the initial tablet erodes, it releases larger sized tablet fragments for tablet B compared with tablet A. These subsequently de-agglomerate or erode, releasing the primary particles which are then available to dissolve. De-agglomeration of clusters of drug particles has been proposed as a possible secondary mechanism (5). Examining the number of particles measured from the QicPic shows no secondary increase in the numbers of particles observed, although the volume based D50 is seen to decrease with time for tablet B (Fig. 6). A secondary de-agglomeration mechanism would further increase the total number of particles following release from the tablet, therefore this mechanism is unlikely in this case. This suggests that the secondary mechanism to be more similar to further erosion and dissolution of fragments for the tablets considered in this paper.

From both the experimental data, and the data fitted modeling approach, it is clear that dissolution rate of a drug substance can be complex. By manipulation of the manufacturing process, tablet "disintegration" and its impact on dissolution can be profoundly affected.

We assert here, that only by measuring and then modeling the relative rates of all the stages of drug

Table IV Fitted Parameters

Parameter	Tablet A	Tablet B
t_ε (min)	1.00	22.1
l_0 (μm)	39.4	69.5
R^2	0.998	0.999

substance dissolution, can a true understanding of the robustness and performance of a tablet formulation be ascertained.

CONCLUSIONS

We have developed a new experimental approach which links tablet disintegration and dissolution into a single measurement framework. The use of a dynamic optical particle imaging approach allows us to measure the number and size of particles which are generated and subsequently evolve during tablet disintegration. Determination of the number and size of particles generated reveals an aspect of tablet behavior which is entirely overlooked by conventional measurement approaches. This new measurement strategy enables us to consider tablet disintegration and dissolution as processes with reaction rates, rather than as simple measures of extents. The consideration of disintegration and dissolution in terms of reaction rates enables us to build the observable tablet performance data into a mechanistic model. The mechanistic framework we chose is the population balance approach, and this has enabled us to incorporate disintegration and dissolution into a single coherent model. We have used this new measurement and modeling approach to describe and understand the performance of two variants of a single formulation which were engineered to give different dissolution behavior. The model shows that the differences in the dissolution performance of the two variants can be described by more fundamental parameters, i.e. differences in initial particle sizes of the dispersed particles and erosion rates of the tablets.

For future work this approach could be expanded to allow for the assessment of particle shape during dissolution and disintegration. This in turn may allow for the identification of specific formulation components.

ACKNOWLEDGMENTS & DISCLOSURES

The authors would like to thank Andrea Moir and Ian Gabbott for analytical support and tablet manufacture. The authors would like to thank Sympatec, UK, for the loan of the LIXELL unit.

REFERENCES

1. Tong C, D'Souza S, Parker J, Mirza T. Commentary on AAPS Workshop. Pharm Res. 2007;24:1603–7.
2. Azarmi S, Roa W, Löbenberg R. Current perspectives in dissolution testing of conventional and novel dosage forms. Int J Pharm. 2007;328:12–21.
3. Donauer N, Löbenberg R. A mini review of scientific and pharmacopeial requirements for the disintegration test. Int J Pharm. 2007;345:2–8.
4. Liu J, Stewart PJ. Deaggregation during the dissolution of benzodiazepines in interactive mixtures. J Pharm Sci. 1998;87:1632–8.
5. Stewart PJ, Zhao F. Understanding agglomeration of indomethacin during the dissolution of micronised indomethacin mixtures through dissolution and de-agglomeration modeling approaches. Eur J Pharm Biopharm. 2005;59:315–23.
6. Zhao F, Stewart PJ. De-agglomeration of micronized benzodiazepines in dissolution media measured by laser diffraction particle sizing. J Pharm Pharmacol. 2003;55:749–55.
7. Coutant CA, Skibic MJ, Doddridge GD, Kemp CA, Sperry DC. *In Vitro* Monitoring of Dissolution of an Immediate Release Tablet by Focused Beam Reflectance Measurement. Mol Pharmaceut. 2010;7:1508–15.
8. Tajarobi F, Abrahmsén-Alami S, Hansen M, Larsson A. The Impact of Dose and Solubility of Additives on the Release from HPMC Matrix Tablets—Identifying Critical Conditions. Pharm Res. 2009;26:1496–503.
9. Laitinen R, Lahtinen J, Silfsten P, Vartiainen E, Jarho P, Ketolainen J. An optical method for continuous monitoring of the dissolution rate of pharmaceutical powders. J Pharm Biomed Anal. 2010;52:181–9.
10. Chew JW, Chow PS, Tan RBH. Automated In-line Technique Using FBRM to Achieve Consistent Product Quality in Cooling Crystallization. Cryst Growth Des. 2007;7:1416.
11. Hermanto MW, Chow PS, Tan RBH. Implementation of Focused Beam Reflectance Measurement (FBRM) in Antisolvent Crystallization to Achieve Consistent Product Quality. Cryst Growth Des. 2010;10:3668–74.
12. Huang J, Kaul G, Utz J, Hernandez P, Wong V, Bradley D, *et al.* A PAT approach to improve process understanding of high shear wet granulation through in-line particle measurement using FBRM C35. J Pharm Sci. 2010;99:3205–12.
13. Ho R, Wilson DA, Heng JYY. Crystal Habits and the variation in surface energy heterogeneity. Cryst Growth Des. 2009;9:4907–11.
14. Sandler N, Wilson D. Prediction of granule packing and flow behavior based on particle size and shape analysis. J Pharm Sci. 2010;99:958–68.
15. USP 28 *Physical Tests*/ <701>Disintegration. United States Pharmacopeia.
16. Randolph AD, Larson MA. Theory of Particulate Processes. Burlington: Academic Press Inc; 1971.
17. Gelbard F, Seinfeld JH. Numerical solution of the dynamic equation for particulate systems. J Comp Phys. 1978;28:357–75.